ELSEVIER

Journal of Nuclear Materials 294 (2001) 193–197

journal of nuclear materials

www.elsevier.nl/locate/jnucmat

Thermal conductivity of $(U,Ce)O_2$ with and without Nd or Zr

Ken Kurosaki [a,*], Ryo Ohshima [a], Masayoshi Uno [a], Shinsuke Yamanaka [a], Kazuya Yamamoto [b], Takashi Namekawa [b]

[a] *Department of Nuclear Engineering, Graduate School of Engineering, Osaka University, Yamadaoka 2-1, Suita, Osaka 565-0871, Japan*
[b] *Alpha-Gamma Section, Fuels and Materials Division, Irradiation Center, Oarai Engineering Center, Japan Nuclear Cycle Development Institute, Narita-cho 4002, Oarai-machi, Ibaraki 311-1393, Japan*

Abstract

The thermal conductivities of $(U_{0.8-x}Ce_{0.2}M_x)O_2$ [M: Nd ($0 \leqslant x \leqslant 0.13$) or Zr ($0 \leqslant x \leqslant 0.06$)] were evaluated from the thermal diffusivity measured by the laser flash method. The thermal conductivities of $(U_{0.8-}Ce_{0.2}M_x)O_2$ indicated a systematic decrease with increasing M-atom content at all temperatures from 200 to 1500 K. In addition, the thermal conductivities of all samples decreased with increasing temperature up to about 1000 K. Up to about 1000 K, the thermal conductivity of $(U_{0.8-x}Ce_{0.2}M_x)O_2$ could be expressed as a function of M-element content by the phonon conduction equation.

1. Introduction

The thermal conductivity of a nuclear fuel under irradiation is very important to evaluate the safety of the fuel. In irradiated uranium–plutonium mixed oxide (MOX) fuel for fast breeder reactors (FBR), a number of fission products (FPs) are produced and they affect the physico-chemical properties of the fuel. Some FPs such as zirconium and rare earth elements are dissolved in the matrix phase during irradiation, and they considerably reduce the thermal conductivity of the fuel [1–5]. A number of studies relating the effect of the FPs to the thermal conductivity of the real MOX and UO_2-based SIMFUEL have been carried out [6–22].

The mixed fluorite-type oxide $(U,Ce)O_2$ has often been used as simulated MOX fuel because of its similar chemical and/or thermodynamic behavior [23–32]. Further, cerium is produced in a nuclear fuel as one of the major FPs and it goes into solid solution in the fuel matrix. Although CeO_2 cannot simulate all the properties of PuO_2 completely, the physico-chemical properties of $(U,Ce)O_2$ will help to understand the properties of MOX fuel to some extent.

In the present study, the effect of the dissolved elements such as Zr or Nd on the thermal conductivity of $(U,Ce)O_2$ are studied, and the results are compared with the data of real MOX and UO_2-based SIMFUEL [10,13,22,33]. By using the phonon conduction equation, the thermal conductivities of $(U_{0.8-x}Ce_{0.2}M_x)O_2$ are also expressed as a function of M-atom content.

2. Experimental

$(U_{0.8-x}Ce_{0.2}M_x)O_2$ [M: Nd ($0 \leqslant x \leqslant 0.13$) or Zr ($0 \leqslant x \leqslant 0.06$)] pellets were prepared from UO_2, CeO_2, ZrO_2 and Nd_2O_3 powders. Nd and Zr were selected as representatives for the dissolved elements in the fuel matrix. Appropriate amounts of the starting materials were blended together and pressed into pellets, followed by reacting and sintering at 2023 K in flowing $(H_2 + 3N_2)/H_2O$ mixture. The oxygen potential of the sintering atmosphere was −370 kJ/mol at 2023 K. The crystal structure of the samples were analyzed by a powder X-ray diffraction method using a Cu-Kα radiation at room temperature. For thermal conductivity measurements, appropriate disk shapes (1.0 mm in thickness and 10 mm in diameter) were cut from the pellets. The densities of the samples were calculated from the measured weight and dimensions. In the temperature range from room temperature to about 1500 K,

* Corresponding author. Tel.: +81-6 6879 7905; fax: +81-6 6879 7889.
E-mail address: kurosaki@nucl.eng.osaka-u.ac.jp (K. Kurosaki).

0022-3115/01/$ - see front matter
PII: S0022-3115(01)00458-5

the thermal conductivity was evaluated from the heat capacity, the experimental density, and the thermal diffusivity measured by the laser flash method using ULVAC TC-7000 in vacuum. The heat capacities of $(U_{0.8-x}Ce_{0.2}M_x)O_2$ were evaluated from Neumann–Kopp's law using the literature data [34] of UO_2, CeO_2 and Nd_2O_3 or ZrO_2.

3. Results and discussion

The powder X-ray diffraction patterns at room temperature of all the samples show single-phase fluorite-type structure. This indicates that both Nd and Zr are dissolved in the $(U,Ce)O_2$ matrix. The lattice parameter and X-ray density were obtained from the X-ray diffraction analysis. The measured bulk densities of the samples are about 93% of the theoretical X-ray densities.

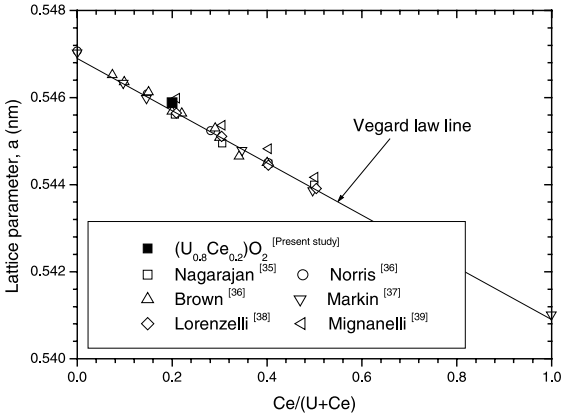

Fig. 1. Comparison of lattice parameters of $(U_{0.8-x}Ce_{0.2})O_2$ obtained in the present study and stoichiometric $(U,Ce)O_{2.00}$ reported in the literature.

Fig. 1 shows the reported lattice parameters of stoichiometric $(U,Ce)O_2$ as a function of cerium content [35–39]. The lattice parameter of $(U_{0.8}Ce_{0.2})O_2$ prepared in the present study satisfies Vegard's law and is close to the previous reported value [35–39] in which the sample composition was nearly stoichiometric. Although the O/M ratio of the samples was not measured chemically, the deviation from the stoichiometry is small. The sample characterizations of $(U_{0.8-x}Ce_{0.2}M_x)O_2$ are shown in Table 1. The lattice parameters of $(U_{0.8-x}Ce_{0.2}Nd_x)O_2$ decrease with increasing Nd content, whereas the lattice parameters of $(U_{0.8-x}Ce_{0.2}Zr_x)O_2$ are almost constant.

The thermal conductivity λ was calculated from the measured thermal diffusivity D, specific heat capacity C_p, and density d using the following relationship:

$$\lambda = DC_p d. \tag{1}$$

The temperature dependence of the thermal conductivities of $(U_{0.8-x}Ce_{0.2}Nd_x)O_2$ and $(U_{0.8-x}Ce_{0.2}Zr_x)O_2$ are shown in Figs. 2 and 3, respectively. These experimental data were normalized to 95% of the theoretical density by using the Maxwell–Eucken relationship [40,41]. The thermal conductivities of $(U_{0.8-x}Ce_{0.2}M_x)O_2$ showed a systematic decrease with increasing M-atom content at all temperatures. In addition the thermal conductivities of all samples decreased with increasing temperature up to about 1000 K, and then increased slowly when the temperature was further increased.

The thermal conductivity of $(U_{0.7}Ce_{0.2}Nd_{0.1})O_2$ is shown in Fig. 5 together with the data of UO_2, $(U_{0.7}Pu_{0.2}Nd_{0.1})O_2$, 10 at.% burnup $(U_{0.8}Pu_{0.2})O_2$, and UO_2-based 8 at.% SIMFUEL [10,13,22,33] (see Fig. 4). The thermal conductivity of $(U_{0.7}Ce_{0.2}Nd_{0.1})O_2$ is lower than that of both UO_2-based and MOX-based SIMFUEL. This is because the SIMFUEL contains metallic FP inclusions, which give a positive contribution to the thermal conductivity. On the other hand, as

Table 1
X-ray diffraction results and bulk densities of $(U_{0.8-x}Ce_{0.2}M_x)O_2$ (M: Nd or Zr)

Samples content (mol%)			X-ray diffraction results	Bulk densities	
UO_2	CeO_2	$NdO_{1.5}$	Lattice parameters (nm)	g/cm^3	%T.D.
80.0	20.0	0.0	0.54588 ± 0.00009	9.694	94.76
78.0	20.0	2.0	0.54616 ± 0.00016	9.520	93.91
76.0	20.0	4.0	0.54597 ± 0.00016	9.593	95.25
73.0	20.0	7.0	0.54560 ± 0.00013	9.588	96.11
70.0	20.0	10.0	0.54589 ± 0.00011	9.037	91.78
67.0	20.0	13.0	0.54538 ± 0.00016	9.196	94.24
UO_2	CeO_2	ZrO_2	Lattice parameters (nm)	g/cm^3	%T.D.
79.0	20.0	1.0	0.54624 ± 0.00012	9.500	93.61
78.0	20.0	2.0	0.54597 ± 0.00009	9.390	92.93
77.0	20.0	3.0	0.54631 ± 0.00011	9.980	97.56
75.5	20.0	4.5	0.54560 ± 0.00015	9.402	94.26
74.0	20.0	6.0	0.54543 ± 0.00013	9.108	92.06

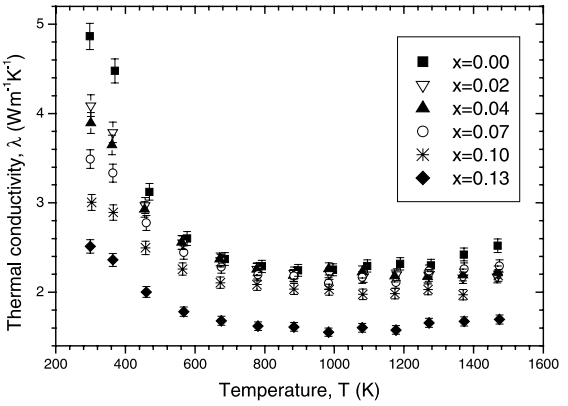

Fig. 2. Thermal conductivity of $(U_{0.8-x}Ce_{0.2}Nd_x)O_2$ as a function of temperature.

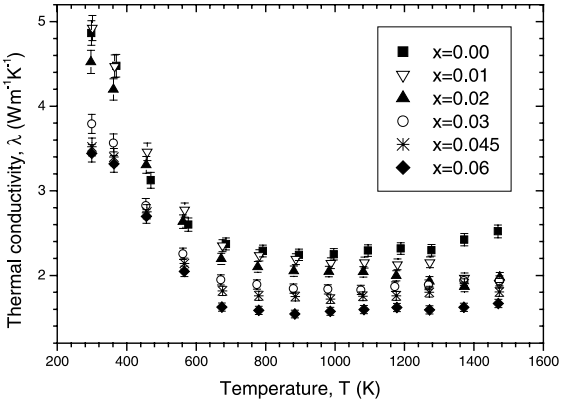

Fig. 3. Thermal conductivity of $(U_{0.8-x}Ce_{0.2}Zr_x)O_2$ as a function of temperature.

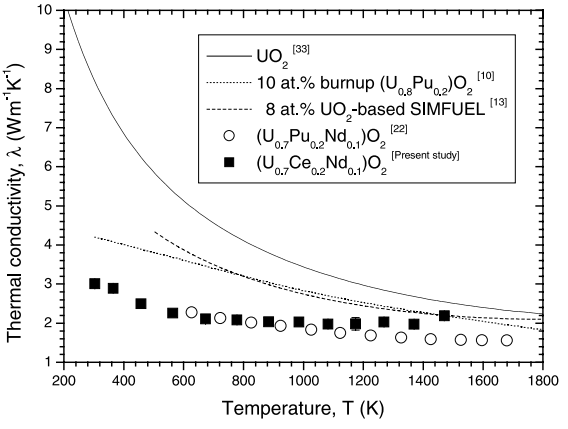

Fig. 4. Comparison of thermal conductivities of $(U_{0.7}Ce_{0.2}Nd_{0.1})O_2$, UO_2, $(U_{0.7}Pu_{0.2}Nd_{0.1})O_2$, 10 at.% burnup $(U_{0.8}Pu_{0.2})O_2$, and UO_2-based 8 at.% SIMFUEL.

seen in this figure, the thermal conductivity of $(U_{0.7}Ce_{0.2}Nd_{0.1})O_2$ nearly equals that of $(U_{0.7}Pu_{0.2}Nd_{0.1})O_2$ up to about 1000 K.

The thermal resistivities W, i.e., the reciprocals of the thermal conductivities, of $(U_{0.8-x}Ce_{0.2}M_x)O_2$ increased linearly with increasing temperature up to about 1000 K, indicating that the thermal conductivity of the samples can be expressed by the following relationship:

$$\lambda = (A + BT)^{-1}, \tag{2}$$

where T is the absolute temperature, and A and B are constants. Values of A and B were determined by fitting the experimental data to Eq. (2) and are shown in Table 2. The values of A increased gradually with increasing M-atom content, while B was almost constant.

When the thermal conduction of dielectric solids is dominated by phonon conduction above its Debye temperature, the thermal resistivity W can be expressed by the following relationship:

$$W = \frac{1}{\lambda} = W_P + W_I. \tag{3}$$

W_P is the intrinsic lattice thermal resistivity caused by phonon–phonon interactions based on the Umklapp process, and corresponds to BT in Eq. (2). W_I is the thermal resistivity resulting from phonon–lattice defect interactions, and corresponds to A in Eq. (2). In addition, W_I of solids can be generally expressed by the following equation:

$$W_I = W_I(0) + \Delta W_I(x). \tag{4}$$

$W_I(0)$ is the lattice defect thermal resistivity caused by the defects such as impurities included in the sample

Table 2
Values of A and B of $(U_{0.8-x}Ce_{0.2}M_x)O_2$ (M: Nd or Zr) determined by fitting the thermal conductivities to $\lambda = (A + BT)^{-1}$ relationship

$NdO_{1.5}$ contents (mol %)	A (mK/W)	B (m/W)
0.00	0.0945	0.0004
0.02	0.1479	0.0004
0.04	0.1619	0.0004
0.07	0.2025	0.0003
0.10	0.2567	0.0003
0.13	0.2966	0.0004
ZrO_2 contents (mol %)	A (mK/W)	B (m/W)
0.00	0.0094	0.0004
0.01	0.0108	0.0006
0.02	0.0271	0.0006
0.03	0.0389	0.0007
0.045	0.053	0.0007
0.06	0.0424	0.0008

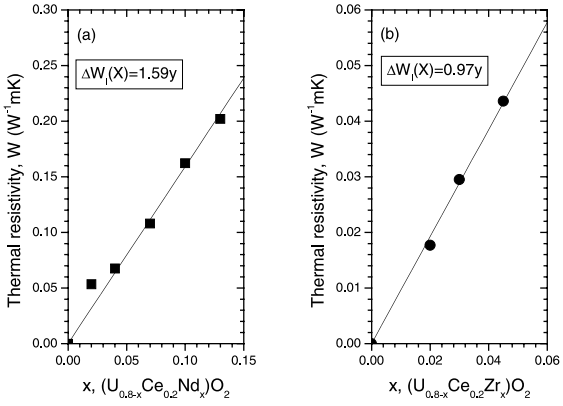

Fig. 5. Relationship between $\Delta W_i(x)$ and M content of $(U_{0.8-x}Ce_{0.2}M_x)O_2$: (a) M = Nd; (b) M = Zr.

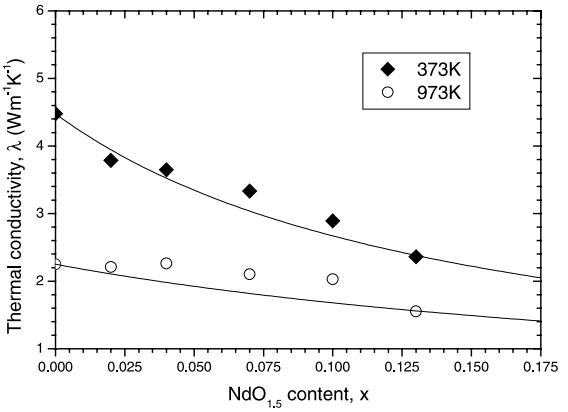

Fig. 6. Comparison between experimental and calculated results of thermal conductivity of $(U_{0.8-x}Ce_{0.2}Nd_x)O_2$.

initially, and corresponds to W_i ($=A$) of $(U_{0.8}Ce_{0.2})O_2$ in the present study. $\Delta W_i(x)$ is the additional defect thermal resistivity caused by dissolution of solutes. In the present study these solutes correspond to M atoms (Nd and Zr). The relationships between $\Delta W_i(x)$ and M-atom content are shown in Fig. 5. The figure shows that $\Delta W_i(x)$ is proportional to the M-atom content.

Since the measured values of B for $(U_{0.8-x}Ce_{0.2}M_x)O_2$ are almost independent of M-atom content, as shown in Table 2, the effect of the intrinsic lattice thermal resistivity W_P on the additional defect thermal resistivity $\Delta W_i(x)$ is negligible. Substituting Eq. (4) into Eq. (3), the following expression for the thermal conductivity of $(U_{0.8-x}Ce_{0.2}M_x)O_2$ can be obtained:

$$\lambda = \frac{1}{W_P(0) + W_i(0) + \Delta W_i(x)}, \tag{5}$$

where $W_P(0)$ is the intrinsic lattice thermal resistivity of $(U_{0.8}Ce_{0.2})O_2$. In addition, the thermal conductivity λ_0 of $(U_{0.8}Ce_{0.2})O_2$ is given by

$$\lambda_0 = \frac{1}{W_P(0) + W_i(0)}. \tag{6}$$

Therefore Eq. (5) becomes

$$\lambda = \frac{\lambda_0}{\Delta W_i(x)\lambda_0 + 1}. \tag{7}$$

Since $\Delta W_i(x)$ is proportional to the M-atom content as described previously, Eq. (7) is expressed by

$$\lambda = \frac{\lambda_0}{kx\lambda_0 + 1}, \tag{8}$$

where k is a constant and x is the M-atom content in $(U_{0.8-x}Ce_{0.2}M_x)O_2$. From Fig. 5, the constants k were found to be 1.59 and 0.97 for Nd and Zr, respectively.

The thermal conductivity of $(U_{0.8-x}Ce_{0.2}Nd_x)O_2$ is shown in Fig. 6 as a function of Nd content. Solid lines correspond to the calculated results obtained from Eq. (8). Although at high temperatures, slight deviations of the experimental data from the calculated results are observed, the thermal conductivity of $(U_{0.8-x}Ce_{0.2}Nd_x)O_2$ can be expressed by using Eq. (8).

4. Summary

The thermal conductivities of $(U_{0.8-x}Ce_{0.2}M_x)O_2$ [M: Nd ($0 \leqslant x \leqslant 0.13$) or Zr ($0 \leqslant x \leqslant 0.06$)] were evaluated in the temperature range from room temperature to about 1500 K. The thermal conductivities decreased gradually with increasing M-atom content. The thermal conductivity of $(U_{0.7}Ce_{0.2}Nd_{0.1})O_2$ was lower than that of both UO_2-based and MOX-based SIMFUEL, but approximately equal to that of $(U_{0.7}Pu_{0.2}Nd_{0.1})O_2$. The thermal conductivities of $(U_{0.8-x}Ce_{0.2}M_x)O_2$ up to about 1000 K could be expressed as a function of M-atom content by the phonon conduction equation.

References

[1] H. Kleykamp, J. Nucl. Mater. 131 (1985) 221.
[2] H. Kleykamp, Nucl. Technol. 80 (1988) 412.
[3] J.H. Davies, F.T. Ewart, J. Nucl. Mater. 41 (1971) 143.
[4] W.D. Kingery, J. Am. Ceram. Soc. 42 (1959) 617.
[5] M. Murabayashi, J. Nucl. Sci. Technol. 7 (1970) 559.
[6] Y. Takahashi, M. Murabayashi, J. Nucl. Sci. Technol. 12 (1975) 133.
[7] R.L. Gibby, J. Nucl. Mater. 38 (1971) 163.
[8] L.A. Goldsmith, J.A.M. Douglas, J. Nucl. Mater. 43 (1972) 225.
[9] D.G. Martin, J. Nucl. Mater. 110 (1982) 73.
[10] Y. Philipponneau, J. Nucl. Mater. 188 (1992) 194.
[11] C. Duriez et al., J. Nucl. Mater. 277 (2000) 143.
[12] P.G. Lucuta, Hj. Matzke, R.A. Verrall, H.A. Tasman, J. Nucl. Mater. 188 (1992) 198.

[13] P.G. Lucuta, Hj. Matzke, R.A. Verrall, J. Nucl. Mater. 217 (1994) 279.
[14] P.G. Lucuta, Hj. Matzke, R.A. Verrall, J. Nucl. Mater. 223 (1995) 51.
[15] P.G. Lucuta, Hj. Matzke, I.J. Hastings, J. Nucl. Mater. 232 (1996) 166.
[16] S. Fukushima, T. Ohmichi, A. Maeda, H. Watanabe, J. Nucl. Mater. 102 (1981) 30.
[17] S. Fukushima, T. Ohmichi, A. Maeda, H. Watanabe, J. Nucl. Mater. 102 (1981) 40.
[18] S. Fukushima, T. Ohmichi, A. Maeda, H. Watanabe, J. Nucl. Mater. 105 (1982) 201.
[19] S. Fukushima, T. Ohmichi, A. Maeda, M. Handa, J. Nucl. Mater. 114 (1983) 260.
[20] S. Fukushima, T. Ohmichi, A. Maeda, M. Handa, J. Nucl. Mater. 114 (1983) 312.
[21] S. Fukushima, T. Ohmichi, A. Maeda, M. Handa, J. Nucl. Mater. 115 (1983) 118.
[22] S. Fukushima, T. Ohmichi, A. Maeda, M. Handa, J. Nucl. Mater. 116 (1983) 287.
[23] R. Ducroux, Ph.J. Baptiste, J. Nucl. Mater. 97 (1981) 333.
[24] Y.S. Park, H.Y. Sohn, D.P. Butt, J. Nucl. Mater. 280 (2000) 285.
[25] D.R. Lide, Handbook of Chemistry and Physics, 77th Ed., CRC, New York, 1996&1997.
[26] L.R. Morss, J. Fuger, Transuranium Elements, American Chemical Society, Washington, DC, 1992.
[27] A. Nakamura, J. Nucl. Mater. 201 (1993) 17.
[28] O. Toffsorensen, J. Solid-State Chem. 18 (1976) 217.
[29] C. Guminski, Z. Metallkd. 81 (1990) 105.
[30] P. Kofstad, Nonstoichiometry, Diffusion, and Electrical Conductivity in Binary Metal Oxides, vol. 276, Wiley–Interscience, New York, 1972.
[31] J.L. Smith, Z. Fisk, S.S. Hecker, Physica B 130 (1985) 151.
[32] G.V. Samsonov, The Oxide Handbook, IFI/Plenum Data, New York, 1973.
[33] MATPRO-Version 11 (Revision 2), NUREG/CR-0497, TREE-1280, Rev. 2, August 1981.
[34] Japan Thermal Measurement Society, Thermodynamics data base for personal computer MALT2.
[35] K. Nagarajan et al., J. Nucl. Mater. 130 (1985) 242.
[36] D.I.R. Norris, P. Kay, J. Nucl. Mater. 116 (1983) 184.
[37] T.L. Markin, R.S. Street, J. Inorg. Nucl. Chem. 32 (1970) 59.
[38] R. Lorenzelli, B. Touzellin, J. Nucl. Mater. 95 (1980) 290.
[39] M.A. Mignanelli, P.E. Potter, J. Nucl. Mater. 118 (1983) 150.
[40] J.C. Maxwell, Treaties on Electricity and Magnetism, vol. 1, 3rd Ed., Oxford University, London, 1891 (reprinted by Dover, New York, 1954).
[41] A.E. Eucken, Forsch. Gebiete Ingenieurw. B3, Forschungsheft, 353, 1932, 16.